Journal of Colloid and Interface Science 362 (2011) 1–4

Contents lists available at ScienceDirect

Journal of Colloid and Interface Science

www.elsevier.com/locate/jcis

Multi-lamellar vesicle formation in a long-chain nonionic surfactant: $C_{16}E_4/D_2O$ system

Luigi Gentile [a,*], Kell Mortensen [b], Cesare Oliviero Rossi [a], Ulf Olsson [c], Giuseppe A. Ranieri [a]

[a] Department of Chemistry, University of Calabria, via P. Bucci, cubo 14C, 87036 Rende, Italy
[b] Nanobioscience Group, IGM-LIFE, University of Copenhagen, Frederiksberg, Denmark
[c] Physical Chemistry 1, Kemicentrum, Lund University, Box 124, 221 00 Lund, Sweden

ARTICLE INFO

Article history:
Received 18 May 2011
Accepted 21 June 2011
Available online 2 July 2011

Keywords:
C_nE_m
Rheology
Rheo-SANS
Rheo-NMR
MLV formation

ABSTRACT

The temperature dependent rheological and structural behavior of a long-chain $C_{16}E_4$ (tetraethylene glycol monohexadecyl ether) surfactant in D_2O has been studied within the regime of low shear range. In the absence of shear flow, the system forms a lamellar liquid crystalline phase at relatively high temperatures. The present paper reports on the shear-induced multi-lamellar vesicle (MLV) formation in $C_{16}E_4/D_2O$ at 40 wt.% of surfactant in the temperature range of 40–55 °C. The transition from planar lamellar structure to multi-lamellar vesicles has been investigated by time-resolved experiments combining rheology and nuclear magnetic resonance (rheo-NMR), rheo small-angle neutron scattering (rheo-SANS) and rheometry. The typical transient viscosity behavior of MLV formation has been discovered at low shear rate value of 0.5 s^{-1}.

1. Introduction

Shear-induced structures and structural changes in complex fluids are interesting and important topics in colloidal sciences [1–10]. An example is the stability of multi-lamellar vesicles (MLVs) upon shearing and temperature variations [11,12]. Knowledge about the MLV formation mechanism is important for various applications, which often depend on the viscosity and rely on the vesicle structures. Closed bilayer structures, such as MLVs, are useful to encapsulate drugs, proteins and DNA [13]. The rheological properties of lyotropic liquid crystal phases are often affected by their mechanical history, as the lamellar phase structure show a rich variety of shear-induced orientation states. These shear-induced structures in lamellar phases are often summarized in the so-called orientation diagrams first introduced by Roux and co-workers [14]. MLVs often occur when a defective lamellar phase is subject to a shear flow. The formation of MLVs is accompanied by a shear thickening. By increasing the shear rate further, shear thinning is caused in the MLV region as the MLVs become smaller [3,14]. When the shear rate is increased, some layers are stripped off and this causes a decreasing of the size of MLVs which may vary from hundreds of nanometers to tens of micrometers. Obviously the vesicle number density increases and the total bilayer area can be considered constant [12]. Shear-induced MLVs can be stable for a long time, but they do not correspond to the thermodynamic equilibrium structure of the lamellar system [15–18]. Combining different structural techniques such as X-ray, neutron and light scattering, and NMR (all of these rheo tools equipped), make it possible to investigate fluid structures under flow like MLVs [1–3,8–30] and to determine their characteristic dimensions [10–12,18,20,22–30].

In many nonionic surfactant aqueous systems of the C_nE_m type ($C_nH_{2n+1}(OC_2H_4)_mOH$) a lamellar phase occurs over a wide temperature and concentration range. Within this phase region, a relatively limited area exists where MLVs can be formed by shear. Although a large literature on MLV formation in C_nE_m (with $n = 10$ or 12) water systems has been produced [9,11,12,15,18–23,26], not so much attention has been given to the study of the long-chain systems (i.e. $n = 16$) [28,29].

In the present article the mechanism of the MLV formation has been studied for the long-chain surfactant $C_{16}E_4$, when dissolved in D_2O. At the temperature of 55 °C and at constant shear rate of 0.5 s^{-1}, the system does show a complete MLV formation while a coexistence region of MLVs and planar lamellae occurs at 40 °C applying the same shear rate. Consequently, we observed that temperature causes an inverse effect respect to surfactant with shorter chains ($C_{10}E_3$ and $C_{12}E_4$).

We also found an intermediate multi-lamellar cylinders (MLCs) state, in agreement with earlier studies on C_nE_m/D_2O systems [22,23].

* Corresponding author.
E-mail address: luigi.gentile@unical.it (L. Gentile).

0021-9797/$ - see front matter © 2011 Elsevier Inc. All rights reserved.
doi:10.1016/j.jcis.2011.06.053

2. Materials and methods

2.1. Materials

Tetra-ethyleneglycol mono hexa-decyl ether ($C_{16}E_4$) has been used as surfactant with a 40.0 ± 0.2 wt.% concentration in D_2O. $C_{16}E_4$ has been purchased from Nikko Chemicals Co., Ltd. (Tokyo, Japan); D_2O has been purchased from Armar Chemicals. Both materials have a declared purity higher than 99.8%, and have been used without further purification. Samples have been prepared by simply mixing surfactant and D_2O, helped by gentle shaking, and left overnight. Normally this is sufficient to yield a homogeneous lamellar phase at 40 °C.

2.2. Rheo-small angle neutron scattering (SANS)

Small-angle neutron scattering experiments have been performed on the SANS-II instrument at the SINQ, Paul Scherrer Institute, Switzerland [31]. Time-resolved neutron scattering experiments have been carried out in a q-range of 0.02–0.35 Å^{-1}, while the sample has been subjected to shear using a couette cell with an inner rotating cylinder of 14 mm radius, and a gap equal to 1 mm. The shear cell was mounted in radial beam position, with the neutron beam passing through the sample along the velocity gradient direction, i.e. the scattering is observed in the plane expanded by the flow and the vorticity (neutral) directions perpendicular to the shear-gradient [32].

The shear rate was calculated using $\dot{\gamma} = 2\pi\Omega(R)(R_0 - R_1)$, where Ω is the angular velocity, R_1=14 mm and R_0 = 15 mm are the inner and outer radii respectively, and $R = (R_0 + R_1)/2$.

The data have been corrected for background and empty cell scattering according to the standard procedure. The high temperatures and the long time of the experiments forced us to paid particular attention to control solvent evaporation as the accuracy of the temperature control is ±0.1 °C. In the rheo-SANS experiments the evaporation was avoided by using a sealed couette.

2.3. Rheo-nuclear magnetic resonance (NMR)

The rheo-^{2}H NMR experiments have been carried out using a cylindrical couette cell (9 mm inner radius, and 1 mm gap). This cell is integrated into an NMR microimaging probe for a wide-bore superconducting magnet. The axis of the shear cell is aligned parallel to the magnetic field. Shear is applied by rotating the inner cylinder with an external stepper-motor gearbox assembly mounted on top of the NMR magnet. The spectra were recorded with a Bruker Avance 300 (Bruker, Germany) operating at a deuterium resonance frequency of 46.073 MHz. The evaporation was avoided by using a sealed couette. Temperature was strictly controlled (±0.2 °C).

The ^{2}H NMR technique probes the motionally averaged electric quadrupole couplings between the deuterium nuclei (spin I = 1) and the electric field gradients at the sites of the observed nuclei [33]. In the case of uniaxial symmetry, as for the lamellar phase, the ^{2}H spectrum consists of a doublet with a frequency separation $\Delta\nu$ given by [33,34] $\Delta\nu = \frac{3}{4}\delta(\cos^2\theta - 1)$, where θ is the angle between the director (the symmetry axis of the phase) and the magnetic field and δ is the motionally averaged quadrupole coupling constant.

2.4. Rheology

The $C_{16}E_4/D_2O$ system is very sensitive to the applied mechanical history and for this reason we have performed the rheological measurements in triplicate with a stress controlled rheometer. The rheology experiments have been performed on a Physica UDS 200 rheometer using the cylindrical geometry (Z3 DIN, inner radius 12.5 mm, gap 1 mm). In addition the rheometer has been equipped with evaporation trap and temperature control of ±0.1 °C.

3. Results and discussion

3.1. Shear-induced transition in $C_{16}E_4/D_2O$ system

The time-dependent transient viscosity for a 40 wt.% $C_{16}E_4/D_2O$ system measured at 40 °C is shown in Fig. 1. The viscosities have been measured applying different shear rate values. It is remarkable to note: (i) high viscosity values at low shear rate values, in comparison with other C_nE_m surfactants [21]; (ii) a significant increase in viscosity is observed at shear rate of 0.5 s^{-1}.

The triplicate experiments show a similar behavior of the viscosity and they reach a viscosity steady state value in the error range of ±0.5 Pa s, Table 1.

The increase of viscosity likely denotes the formation of MLV as a result of the shear, even though the viscosity is not as high as that usually observed in the mechanism of the MLV formation [15,21]. The small increase of viscosity may be interpreted in terms of coexistence of MLV and lamellar phases. The MLV formation is further confirmed by rheo-NMR experiments shown in Fig. 2. In fact the characteristic "Pake" doublet of the planar lamellae turns into a broad single peak as a consequence of the MLVs presence [19,20]. After 30,000 s under shear rate of 0.5 s^{-1} no substantial modifications have been observed on the spectra as it is possible to see in the inset B in Fig. 2. Moreover the NMR line shape of the spectra seems to confirm the MLV and lamellar phases coexistence.

The same experiments have been performed at 55 °C and the transient viscosities, applying 0.1, 0.2 and 0.5 s^{-1} shear rates, are shown in Fig. 3. The typical strain evolution of the complete MLV formation [15,21] is reported at 0.5 s^{-1}. On the contrary to what has been observed at 40 °C, the increase in viscosity over time is remarkable and it corresponds to a significant thickening behavior.

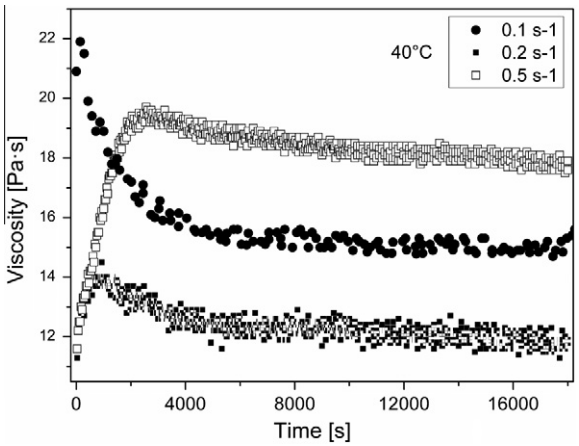

Fig. 1. Transient viscosity under constant shear rates (0.1, 0.2 and 0.5 s^{-1}) of 40 wt.% $C_{16}E_4/D_2O$ system at 40 °C.

Table 1
Steady state viscosity values of the triplicate experiments at 40 °C.

Exp no./shear rates	0.1 s^{-1}	0.2 s^{-1}	0.5 s^{-1}
1	15.0 Pa s	11.9 Pa s	17.8 Pa s
2	15.2 Pa s	11.4 Pa s	17.1 Pa s
3	15.6 Pa s	11.1 Pa s	17.5 Pa s

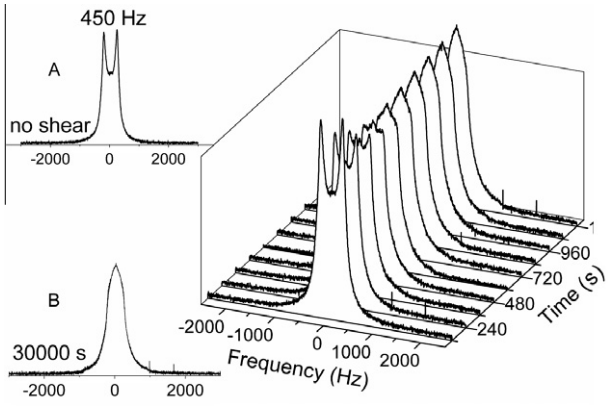

Fig. 2. Time evolution of ^{2}H NMR spectra during the MLV formation from planar lamellae at 40 °C and at constant shear rate of 0.5 s^{-1}. The inset A shows the powder pattern of the lamellar phase with no shear applied. The inset B shows a broad peak attributed to MLV and lamellar phases coexistence after 30,000 s under shear rate of 0.5 s^{-1}.

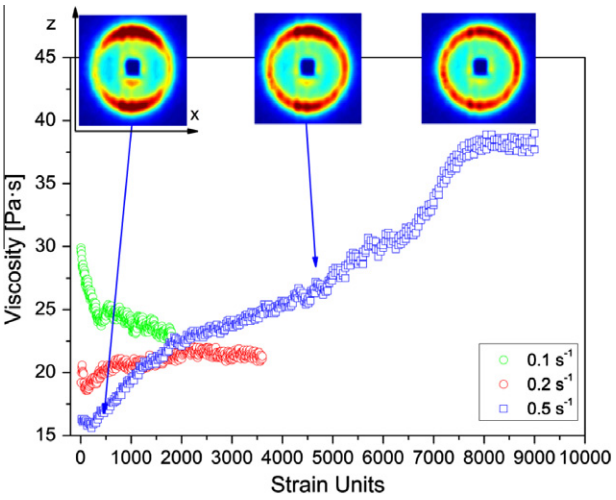

Fig. 3. Transient viscosity under constant shear rates of 40 wt.% $C_{16}E_4$ sample at 55 °C and relative SANS patterns for the transient viscosity obtained at 0.5 s^{-1} at different times (strain units). Anisotropic 2D-scattering patterns have been recorded in vorticity-flow (z–x) plane. The neutron beam passing through the sample along the velocity gradient (y) direction.

The triplicate experiments show a similar behavior of the viscosity and they reach a viscosity steady state value in the error of ±0.7 Pa s.

SANS experiments have been performed at low shear rate values within the q-range 0.02 $Å^{-1} < q < 0.15$ $Å^{-1}$ where the first order Bragg peak, observed at $q \approx 0.09$ $Å^{-1}$, corresponds to the bilayer spacing (d) of 6.9 nm. On the other hand at 40 °C a bilayer spacing of 7.2 nm is observed and this temperature dependence behavior of d-spacing is similar to the data on $C_{16}E_6/D_2O$ found by Penfold et al. [35]. SANS spectra in the radial direction (perpendicular to the direction of flow) have been recorded at intervals of 180 s, with an acquisition time of 1 s. At the shear rate of 0.5 s^{-1} and after 360 s (180 strain units) a pronounced anisotropic scattering is observed (Fig. 3).

The observed peak structure factor at lower strain value, arises likely from a minor population of bilayers with their normal parallel to vorticity direction (z) which is called "a" orientation [36]. However according to the reference [30], the "a" orientation is attributed to a metastable state and it is reasonable to affirm that part of the bilayers orient with their normal parallel to the velocity direction (y), "c" orientation.

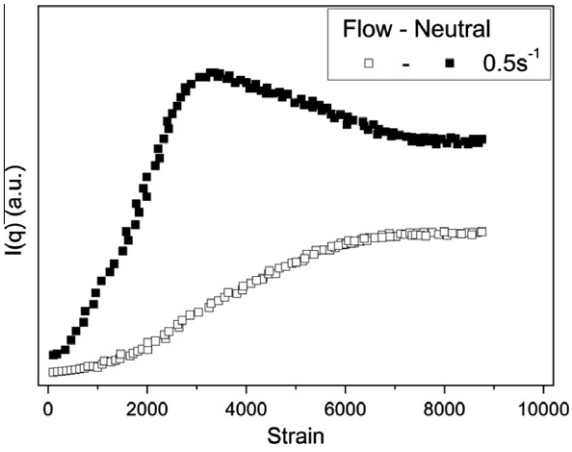

Fig. 4. Evolution of SANS intensity at the lamellar Bragg peak in neutral and flow direction in the radial beam at the shear rate value of 0.5 s^{-1}.

SANS patterns change from the anisotropic pattern to the isotropic ring in time. These changes clearly demonstrate the formation of the isotropic MLVs. In fact the pronounced increase of viscosity due to the mechanism of MLV formation, occurs between 4000 and 9000 strain units.

Usually the pathway of MLV formation reveals a characteristic sequence of lamellae morphology changes. A pre-aligned lamellar phase in the "c" orientation first undergoes to changes into multi-lamellar cylinders (MLCs) followed by MLVs [22,23].

3.2. Intermediate structure during the MLV formation

Fig. 4 shows the peak intensities along the neutral and the flow directions plotted vs. the strain. The data reflect the gradual formation of MLVs in the system. The intensity in the neutral direction reveals a maximum at around 3200 strain units (Fig. 4). This maximum may be due to multilamellar cylinder (MLC) formation as observed previously in the analogous $C_{10}E_3$ and $C_{12}E_4$ systems [23]. Further investigations, including tangential rheo-SANS and rheo-SALS are, however, required to conclusively determine the presence of this intermediate cylinder state. The observation that some anisotropy remains in the SANS patterns after steady state has been reached at approximately 8000 strain units may indicate that either (i) cylinders are still present, (ii) the vesicles are significantly elongated or (iii) planar lamellae are still present.

3.3. Size determination of shear-induced MLVs by rheo-NMR

In Fig. 5 the ^{2}H NMR line shape of heavy water in MLV system at 55 °C is analyzed quantitatively as reported in literature [18], through which the MLV size can be determined. In first approximation the radius of the MLVs determined from the line shape simulation is around 3 μm. A quadrupolar splitting of 480 Hz has been measured. The d-spacing of the bilayer is determined by SANS profile measured without shear rate, d = 6.9 nm. Taking into account the approximations introduced, further investigations are needed to determine the exact MLV radius.

3.4. Temperature effect on the MLV formation

Both temperature and the surfactant chain length are parameters that control the transition from planar lamellae to MLVs. Considering the literature data for the short-chain C_nE_m aqueous systems [23] upon increasing the temperature (changing the spontaneous curvature of the bilayer) at a constant shear rate, a coexis-

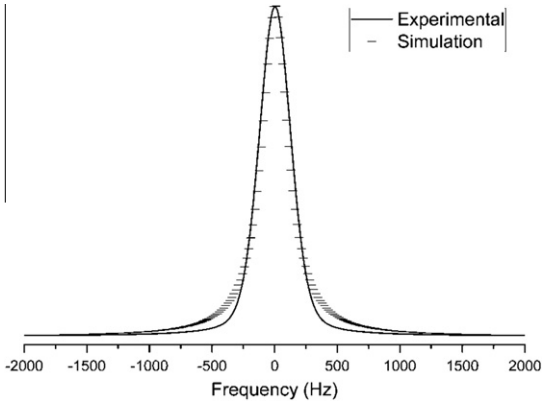

Fig. 5. The Lorentzian line shape simulation on the broad NMR peak of the MLVs. The broad peak has been recorded at 8000 strain units (shear rate 0.5 s^{-1}).

tence region of MLVs and planar lamellae occurs. In $C_{16}E_4/D_2O$ system the temperature has a marked effect on MLV formation, indeed a MLV phase occurs at high temperature, while at lower temperature we observe a regime of MLVs and planar lamellae coexistence. Furthermore in this system the temperature influences the strain required for the MLV formation. In fact the strain required at 40 °C is 2500 strain units (Fig. 1), while it is 8000 strain units at 55 °C (Fig. 3).

This is interpreted in terms of a higher bending rigidity of bilayers, in lamellar phase, of the C_nE_m with shorter chains. By changing the spontaneous curvature of the bilayer (i.e. increasing the temperature), the applied shear flow is able to bend the lamellar bilayers. The assumption of the higher bending rigidity of $C_{16}E_4$ can be made considering the literature [37]. In fact it has been observed that a higher value of "*n*" corresponds to a higher value of bending rigidity, while the systems show an inverse relationship with "*m*".

4. Conclusions

Combined studies of rheology, rheo-NMR and rheo-SANS have revealed that 40 wt.% $C_{16}E_4/D_2O$ system forms a MLV phase when a shear rate of the order of 0.5 s^{-1} is applied. At approximately 8000 strain units the MLV formation is complete at the temperature of 55 °C, while at 40 °C the mechanism was complete reaching the 2500 strain units although with a lamellar phase coexistence. The same does not hold true for the short-chain C_nE_m water systems, which exhibit an opposite trend with the temperature [23]. This temperature effect is connected to the bending rigidity of bilayers in lamellar phase. In particular bilayer rigidity of long-chain surfactants can be considered higher than the short-chain (like $C_{10}E_3$ and $C_{12}E_4$) surfactants [37]. Our results show a similar behavior in temperature to $C_{16}E_7$ studied by Kosaka et al. [29]. Additional studies on long-chain C_nE_m surfactants are needed in order to fully understand the temperature dependence of the MLV formation.

Comparing our results with those of Nettesheim et al. [23] and Gentile et al. [15], we conclude that, for $C_{16}E_4$, $C_{12}E_5$, $C_{12}E_4$ and $C_{10}E_3$ water systems, the transition from planar lamellae to MLVs follows a similar path, except for the temperature dependence of the strain. Comparing the strain values needed for the MLV formation, we note that the $C_{16}E_4$ requires a higher strain than $C_{12}E_5$, while a lower strain than $C_{12}E_4$ and $C_{10}E_3$. This comparison is made at 55 °C for $C_{16}E_4$ and $C_{12}E_5$ and at 25 °C for $C_{12}E_4$ and $C_{10}E_3$.

In the present article we focused on the presence of the lamellar-to-MLV transition in a long-chain nonionic surfactant $C_{16}E_4$ at 40 wt.% in D_2O at low shear rate values. Moreover it was found an inverse temperature relation of the MLV formation compared to the short-chain nonionic surfactant.

Acknowledgments

We would like to thank Dr. Bruno Silva for theoretical and practical assistance and the Paul Scherrer Institute (PSI) for allowing to use their SINQ facility (Instrument: SANS-II, Proposal: 20091327). This research project has been supported by the European Commission under the 7th Framework Programme through the 'Research Infrastructures' action of the 'Capacities' Programme, Contract No: CP-CSA_INFRA-2008-1.1.1 Number 226507-NMI3, and DANSCATT (Danish Natural Research Council).

References

[1] P. Butler, Curr. Opin. Colloid Interface Sci. 4 (1999) 214.
[2] W. Richtering, Curr. Opin. Colloid Interface Sci. 6 (2001) 446.
[3] K. Mortensen, Curr. Opin. Colloid Interface Sci. 6 (2001) 140.
[4] D. Spain, S. Troost, M. Golombok, J. Colloid Interface Sci. 338 (2009) 261.
[5] J. Delgado, R. Castillo, J. Colloid Interface Sci. 312 (2007) 481.
[6] S. Lin-Gibson, H. Kim, G. Schmidt, C.C. Han, E.K. Hobbie, J. Colloid Interface Sci. 274 (2004) 515.
[7] J.G. Watterson, M.C. Schaub, J. Colloid Interface Sci. 45 (1973) 280.
[8] L. Coppola, L. Gentile, I. Nicotera, C. Oliviero Rossi, G.A. Ranieri, Langmuir 26 (2010) 19060.
[9] L. Filippelli, B. Medronho, C. Oliviero Rossi, M.G. Miguel, U. Olsson, Mol. Cryst. Liq. Cryst. 500 (2009) 166.
[10] P. Panizza, A. Colin, C. Coulon, D. Roux, Eur. Phys. J. B 4 (1998) 65.
[11] Y. Suganuma, M. Imai, T. Kato, U. Olsson, T. Takahashi, Langmuir 26 (2010) 7988.
[12] B. Medronho, S. Fujii, W. Richtering, M.G. Miguel, U. Olsson, Colloid Polym. Sci. 284 (2005) 317.
[13] A. Nath, W.M. Atkins, S.G. Sligar, Biochemistry 46 (2007) 2059.
[14] D. Roux, F. Nallet, O. Diat, Europhys. Lett. 24 (1993) 53.
[15] L. Gentile, C. Oliviero Rossi, U. Olsson, G.A. Ranieri, Langmuir 27 (2011) 2088.
[16] M. Gradzielski, J. Phys.: Condens. Matter 15 (2003) 655.
[17] J.I. Escalante, M. Gradzielski, H. Hoffmann, K. Mortensen, Langmuir 16 (2000) 8653.
[18] B. Medronho, C. Schmidt, U. Olsson, M.G. Miguel, Langmuir 26 (2010) 1477.
[19] B. Medronho, S. Shafaei, R. Szopko, M.G. Miguel, U. Olsson, C. Schmidt, Langmuir 24 (2008) 6480.
[20] S. Müller, C. Börschig, W. Gronski, C. Schmidt, D. Roux, Langmuir 15 (1999) 7558.
[21] C. Oliviero, L. Coppola, R. Gianferri, I. Nicotera, U. Olsson, Colloids Surf., A 228 (2003) 85.
[22] J. Zipfel, F. Nettesheim, P. Lindner, T.D. Le, U. Olsson, W. Richtering, Europhys. Lett. 53 (2001) 335.
[23] F. Nettesheim, J. Zipfel, U. Olsson, F. Renth, P. Lindner, W. Richtering, Langmuir 19 (2003) 3603.
[24] J. Bergenholtz, N.J. Wagner, Langmuir 12 (1996) 3122.
[25] J. Läuger, R. Weigel, K. Berger, K. Hiltrop, W. Richtering, J. Colloid Interface Sci. 181 (1996) 521.
[26] L. Courbin, J.P. Delville, J. Rouch, P. Panizza, Phys. Rev. Lett. 89 (2002) 148305.
[27] T.D. Le, U. Olsson, K. Mortensen, Phys. Chem. Chem. Phys. 3 (2001) 1310.
[28] T. Kato, K. Miyazaki, Y. Kawabata, S. Komura, M. Fujii, M. Imai, J. Phys.: Condens. Matter 17 (2005) S2923.
[29] Y. Kosaka, M. Ito, Y. Kawabata, T. Kato, Langmuir 26 (2010) 3835.
[30] T.D. Le, U. Olsson, K. Mortensen, J. Zipfel, W. Richtering, Langmuir 17 (2001) 999.
[31] P. Strunz, K. Mortensen, S. Janssen, Physica B 350 (2004) E783.
[32] K. Mortensen, K. Almdal, F.S. Bates, K. Koppi, M. Tirell, B. Nordén, Physica B 213–214 (1995) 682.
[33] A. Abragam, Principles of Nuclear Magnetism, Clarendon Press, Oxford, 1961.
[34] B. Halle, H. Wennerstrom, J. Chem. Phys. 75 (1981) 1928.
[35] J. Penfold, E. Staples, A. Khan Lodhi, I. Tucker, G.J.T. Tiddy, J. Phys. Chem. B 101 (1997) 66.
[36] C.R. Safinya, E.B. Sirota, R.F. Bruinsma, C. Jeppesen, R.J. Plano, Science 261 (1993) 588.
[37] E. Kurtisovski, N. Taulier, R. Ober, M. Waks, W. Urbach, Phys. Rev. Lett. 98 (2007) 258103.